An assessment of DFT methods for predicting the thermochemistry of ion–molecule reactions of group 14 elements (Si, Ge, Sn)

ARTICLE *in* JOURNAL OF MOLECULAR MODELING · NOVEMBER 2013

Impact Factor: 1.74 · DOI: 10.1007/s00894-013-2038-y · Source: PubMed

3 AUTHORS, INCLUDING:

Igor S. Ignatyev
Saint Petersburg State University
69 PUBLICATIONS **737** CITATIONS
SEE PROFILE

J. J. López González
Universidad de Jaén
134 PUBLICATIONS **1,138** CITATIONS
SEE PROFILE

J Mol Model (2013) 19:5439–5444
DOI 10.1007/s00894-013-2038-y

ORIGINAL PAPER

An assessment of DFT methods for predicting the thermochemistry of ion-molecule reactions of group 14 elements (Si, Ge, Sn)

Igor S. Ignatyev · Manuel Montejo · Juan Jesús López González

Received: 3 September 2013 / Accepted: 17 October 2013 / Published online: 8 November 2013

Abstract Experimental mass-spectrometry data on thermochemistry of methide transfer reactions $(CH_3)_3M^+ + M'(CH_3)_4 \leftrightarrow M(CH_3)_4 + (CH_3)_3M'^+$ (M, M'=Si, Ge or Sn) and the formation energy of the $[(CH_3)_3Si\text{-}CH_3\text{-}Si(CH_3)_3]^+$ complex are used as benchmarks for DFT methods (B3LYP, BMK, M06L, and ωB97XD). G2 and G3 theory methods are also used for the prediction of thermochemical data. BMK, M06L, and ωB97XD methods give the best fit to experimental data (close to chemical accuracy) as well as to G2 and G3 results, while B3LYP demonstrates poor performance. From the first three methods M06L gives the best overall result. Structures and formation energies of intermediate "mixed" $[(CH_3)_3M\text{-}CH_3\text{-}M'(CH_3)_3]$ complexes not observed in experiment are predicted. Their structures, better described as $M(CH_3)_4\,[M'(CH_3)_3]^+$ complexes, explain their fast decompositions.

Keywords DFT · Group 14 elements · Ion-molecule reactions · Thermochemistry

Introduction

Trimethylsilyl cations $(CH_3)_3Si^+$ are the most abundant products of the electron impact ionization of $(CH_3)_4Si$ [1]. This ion associates with the parent tetramethylsilane molecule to produce the $(CH_3)_7Si^+$ ion [2], that was also observed in the chemical ionization studies of pure tetramethylsilane [3–5]. Albeit the structure of this ion was proposed to contain a Si-Si bond with one silicon atom being pentacoordinated [3], the analysis of experimental data and the quantum chemical study of the $(CH_3)_7Si^+$ ion [6] allowed authors to suggest a structure corresponding to a C_{3h} point group in which a planar methyl group is symmetrically bonded to two $-Si(CH_3)_3$ moieties. This structure was found to be a minimum at both B3LYP/6-311+G(3df,2pd) and QCISD/6-311+G(d,p) levels of theory [6]. The latter level predicts ΔH^0 of the ion association to be −23.2 kcal mol^{-1} in good agreement with the experimental value of −22.3±0.4 kcal mol^{-1} [5]. Similar structure (although with nonplanar central methyl moiety) was found earlier as an intermediate in the potential energy surface of the hydrogen transfer reaction between the SiH_3^+ ion and GeH_4 [7].

Fernández, Uggerud, and Frenking [8] obtained equilibrium structures for the $[H_3M\text{-}CH_3\text{-}MH_3]^+$ ions, where M are Group 1, 2, 13 or 14 (Si, Ge, Sn and Pb) elements. Nevertheless, among structures with methyl groups at M, i.e., $[(CH_3)_3M\text{-}CH_3\text{-}M'(CH_3)_3]^+$, only the equilibrium structure of the "symmetric" $[(CH_3)_3Si\text{-}CH_3\text{-}Si(CH_3)_3]^+$ molecule was obtained by quantum chemical methods [6]. Analogous nonsymmetric ("mixed") structures (M, M′ = Si, Ge, and Sn) were not observed by mass spectrometry. Thus, one of the aims of this work is to predict their structures and to get an insight into the factors that prevent them from experimental identification. Despite the lack of information about the intermediates, there exist thermodynamic experimental data of the $(CH_3)_3M^+ + M'(CH_3)_4 \leftrightarrow M(CH_3)_4 + (CH_3)_3M'^+$ reactions (M, M′ = Si, Ge and Sn), that can be used as experimental benchmarks for the quantum chemical calculations of ion-molecule reactions of group 14 elements. Due to the significant size of the systems, which include methyl derivatives, DFT methods are a reasonable choice for this task.

Resembling other commonly used semilocal and hybrid density functionals, which cannot provide the correct dependence of the dispersion interaction energy on the interatomic distance, the widespread B3LYP method yields large errors in

I. S. Ignatyev
Department of Chemistry, Radiochemistry Laboratory, St. Petersburg State University, St. Petersburg 199034, Russia

M. Montejo · J. J. López González (✉)
Department of Physical and Analytical Chemistry, University of Jaén, Campus "Las Lagunillas", 23071 Jaén, Spain
e-mail: jjlopez@ujaen.es

predicting thermochemical parameters for molecular systems with noncovalent interactions [9–21].

For this reason, we used some of the DFT methods recently developed, such as Thrular's M06L (reported to have the best overall performance of any functional for the study of organometallic thermochemistry [22–28]), the hybrid meta-GGA BMK functional which was reported to be superior to B3LYP and other hybrid functionals for equilibrium properties [29–33] as well as the ωB97XD functional that includes dispersion corrections. Further, G2 and G3 methods, which provide the most accurate predictions of thermochemical parameters, have also been implemented for comparison.

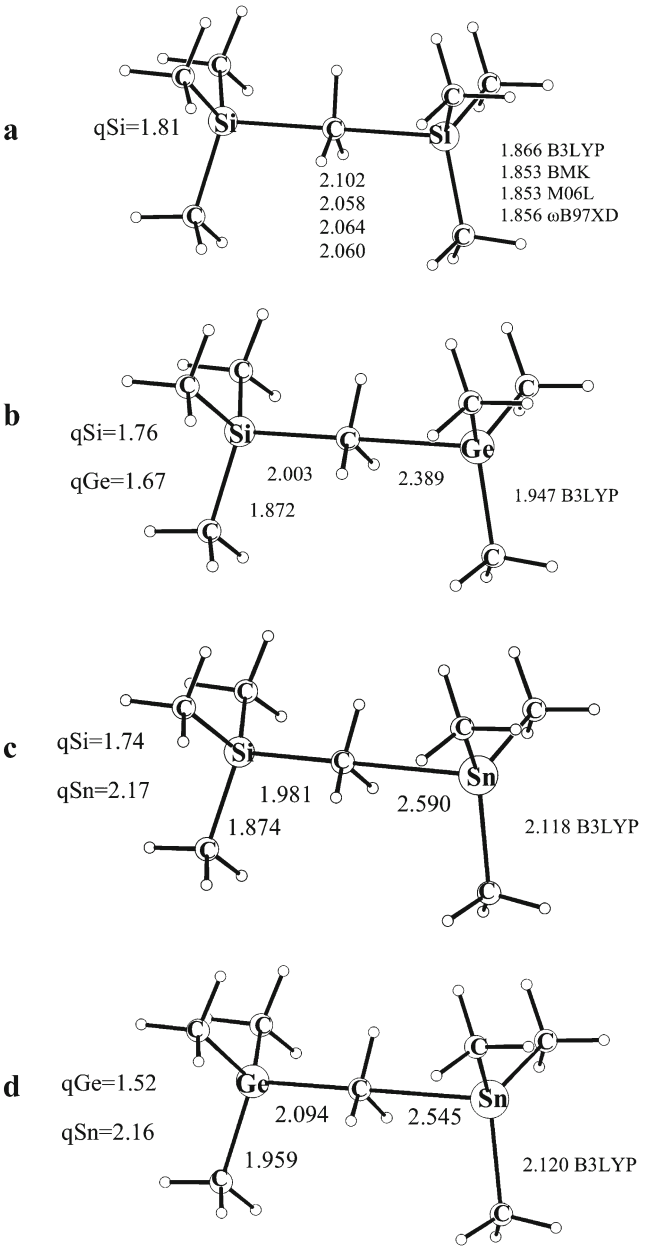

Fig. 1 Structure (bond lengths in Å) of the $(CH_3)_7Si^+$ ion (**a**) and of the intermediates in the methide transfer reactions: $(CH_3)_3M^+ + M'(CH_3)_4 \leftrightarrow (CH_3)_4M' + (CH_3)_3M^+$, where M and M′ denote Si, Ge, and Sn and M≠M′ (**b**, **c**, **d**)

Computational methods

Geometries of stationary points have been fully optimized and characterized by harmonic vibrational frequency calculations using the following DFT methods: (i) the hybrid meta-GGA B3LYP functional [34, 35], (ii) Thrular's pure M06L functional [36], (iii) Boese and Martin's BMK functional [13], and (iv) the long-range corrected (LC) hybrid density functional by Chai and Head-Gordon, with empirical atom–atom dispersion corrections, denominated ωB97X-D [37].

The Dunning correlation-consistent sets [38] were employed for H, C, Si, and Ge atoms. For Sn, a valence double-ζ set with an ECP and relativistic corrections, denominated LANL2DZ [39–41], was used.

G2 [42] and G3 [43] methods were also used for the high-level predictions in cases where experimental thermochemical data were absent.

All the methods and basis sets were used as implemented in the Gaussian09 program [44]. In the DFT methods, the integration was carried out with the Int=Ultrafine option and, for all the methods employed, the geometry optimization criterion used was that corresponding to the Opt=Tight option. Natural bond orbital (NBO) analysis [45, 46] and the counterpoise method [47] for the estimation of basis set superposition errors (BSSE) were also used as implemented in Gaussian09.

Table 1 Theoretical and experimental association energies (ΔH^0 in kcal mol^{-1}) of the $[(CH_3)_3Si\text{-}CH_3\text{-}Si(CH_3)_3]^+$ complex

	cc-pVDZ	aug-cc-pVDZ	cc-pVTZ	aug-cc-pVTZ	aug-cc-pVTZ[a]	BSSE[b]
B3LYP	−17.5	−17.4	−16.5	−16.5		0.3
BMK	−20.8	−21.3	−23.3	−21.4	−20.5	0.5
M06L	−22.6	−23.2	−22.3	−22.0	−22.3	0.7
ωB97XD	−23.9	−24.6	−23.5	−23.4	−23.2	0.3
G2	−23.7					
G2(MP2)	−23.8					
G3	−25.7					
G3(MP2)	−25.4					
Experiment[c]	−22.3±0.4					

[a] Single-point calculation at the B3LYP/aug-cc-pVTZ optimized geometries with thermal correction to enthalpy with the B3LYP method

[b] Basis set superposition error (kcal mol^{-1}) calculated by counterpoise method for B3LYP/aug-cc-pVTZ optimized geometries

[c] Taken from ref [5]

Table 2 Theoretical and experimental enthalpies (ΔH^0 in kcal mol^{-1}) of the $(CH_3)_3Si^+ + (CH_3)_4Ge \leftrightarrow (CH_3)_4Si + (CH_3)_3Ge^+$ reaction

	cc-pVDZ	aug-cc-pVDZ	cc-pVTZ	aug-cc-pVTZ	aug-cc-pVTZ[a]
B3LYP	−7.9	−7.9	−8.3	−8.2	
BMK	−10.0	−10.1	−10.1	−9.9	−10.3
M06L	−9.5	−9.4	−9.6	−9.6	−9.9
ωB97XD	−8.1	−8.1	−8.6	−8.3	−8.3
G2	−9.4				
G2(MP2)	−9.5				
G3	−9.9				
G3(MP2)	−9.3				
Experiment[b]	−10.2±0.6				

[a] Single-point calculation at the B3LYP/aug-cc-pVTZ optimized geometries with thermal correction to enthalpy at the B3LYP level

[b] Taken from ref [5]

Results and discussion

Structure of the intermediate and thermochemistry of the interaction of $(CH_3)_3Si^+$ with $(CH_3)_4Si$

The structure of the adduct formed by the interaction of the trimethylsilylium cation with tetramethylsilane is depicted in Fig. 1(**a**). In accordance with previous optimizations [6], it possesses C_{3h} symmetry. As shown in Fig. 1a, the equilibrium SiC bond distance obtained with aug-cc-pVTZ basis set increases from 2.058 Å (BMK) to 2.102 Å (B3LYP). The highest level QCISD/6-311+G(d,p) equilibrium bond length of 2.071 Å [6] lies in the middle of the range of these values.

Along with the reduction of equilibrium bond lengths, the association energies increase from B3LYP to ωB97XD. The B3LYP values are far from experimental values for all the basis sets employed (see Table 1). Other DFT values provide a good agreement with experimental values as well as with the highest level QCISD estimate (−23.2 kcal mol^{-1}) [6]. The G2 result matches this last value, but is slightly lower than the G3 value (Table 1). Basis set superposition error calculated by the counterpoise method with aug-cc-pVTZ method is small for B3LYP and ωB97XD (0.3 kcal mol^{-1}) and slightly higher for BMK and M06L (0.5 and 0.7 kcal mol^{-1}). Thus, the BSSE-corrected association energy calculated by ωB97XD (−23.1 kcal mol^{-1}) is the closest one to the experimental value (−22.3 kcal mol^{-1}), although the M06L value (−21.6 kcal mol^{-1}) is also close (±1 kcal mol^{-1}) to the experimental result. Note, that B3LYP values demonstrate a small decrease of association energies with the basis set size, while for the other DFT methods the values depend on the basis set to a lesser extent. In Table 1, we also compared the difference of enthalpies calculated with the largest aug-cc-pVTZ set at the optimized geometry obtained by the same method and at geometries of B3LYP. These differences within M06L and ωB97XD are very small (they are slightly larger for BMK). Due to the convergence problems in optimizing the geometries of lower symmetry structures with this extended basis set in the subsequent calculations of "mixed" intermediate complexes we used energy values estimated at the B3LYP/aug-cc-pVTZ geometry.

Thermochemistry of the $(CH_3)_3M^+ + M'(CH_3)_4 \leftrightarrow (CH_3)_4M' + (CH_3)_3M^+$ methide transfer reaction

Since tricoordinated germanium cations are more stable than their silicon analogues [34], reactions $(CH_3)_3M^+ + M'(CH_3)_4 \leftrightarrow (CH_3)_4M' + (CH_3)_3M^+$, with M′ lying lower down the group than M, are exothermic. The accurate values of their enthalpies, obtained by mass-spectrometry [5], may be a benchmark for DFT methods.

The values predicted for the enthalpy of the $(CH_3)_3Si^+ + (CH_3)_4Ge \leftrightarrow (CH_3)_4Si + (CH_3)_3Ge^+$ reaction by the four DFT methods and the aug-cc-pVTZ basis set are ca. 2 kcal mol^{-1}

Table 3 Theoretical and experimental enthalpies (ΔH^0 in kcal mol^{-1}) of the $(CH_3)_3Ge^+ + (CH_3)_4Sn \leftrightarrow (CH_3)_4Ge + (CH_3)_3Sn^+$ reaction

	cc-pVDZ	aug-cc-pVDZ	cc-pVTZ	aug-cc-pVTZ	aug-cc-pVTZ[a]
B3LYP	−5.7	−8.2	−7.9	−7.8	
BMK	−7.2	−9.6	−8.0	−9.4	−9.2
M06L	−5.5	−7.9	−6.6	−7.8	−7.9
ωB97XD	−6.5	−9.2	−8.5	−9.4	−9.2
Experiment[b]	−8.1±0.5				

[a] Single-point calculation at the B3LYP/aug-cc-pVTZ optimized geometries with thermal correction to enthalpy at the B3LYP level

[b] Taken from ref [5]

Table 4 Theoretical and experimental enthalpies (ΔH^0 in kcal mol^{-1}) of the $(CH_3)_3Si^+ + (CH_3)_4Sn \leftrightarrow (CH_3)_4Si+(CH_3)_3Sn^+$ reaction

	cc-pVDZ	aug-cc-pVDZ	cc-pVTZ	aug-cc-pVTZ	aug-cc-pVTZ[a]
B3LYP	−13.7	−16.1	−15.6	−16.0	
BMK	−17.2	−19.6	−18.1	−19.3	−19.5
M06L	−15.0	−17.3	−16.2	−17.4	−17.8
ωB97XD	−14.6	−17.2	−17.1	−17.7	−17.2
Experiment[b]	−18.4				

[a] Single-point calculation at the B3LYP/aug-cc-pVTZ optimized geometries with thermal correction to enthalpy at the B3LYP level

[b] Taken from ref [5]

deviated from experimental values and from those obtained using quantum chemistry composite methods (G2 and G3), as shown in Table 2. Remarkably, M06L and BMK values show an excellent agreement with experiment.

Also considering the results obtained with the aug-cc-pVTZ basis set, for the $(CH_3)_3Ge^+ + (CH_3)_4Sn \leftrightarrow (CH_3)_4Ge+(CH_3)_3Sn^+$ reaction both B3LYP and M06L predictions agree well with experiment (G-theory is unavailable for tin), while BMK and ωB97XD slightly overestimate reaction enthalpies as reported in Table 3. Nevertheless, as in the $(CH_3)_3Si^+ + (CH_3)_4Ge \leftrightarrow (CH_3)_4Si+(CH_3)_3Ge^+$ reaction, all methods are ca. 2 kcal mol^{-1} deviated from experiment.

As concerns the $(CH_3)_3Si^+ + (CH_3)_4Sn \leftrightarrow (CH_3)_4Si+(CH_3)_3Sn^+$ reaction, it has the highest value of ΔH^0 for the studied methide transfer process, i.e., −18.4 kcal mol^{-1} [5]. Again, M06L, BMK and ωB97XD values are in good agreement with experiment (deviations of ca. 2 kcal mol^{-1} from experiment, when using aug-cc-pVTZ basis set), while the B3LYP value is underestimated (2.4 kcal mol-1 far from the experimental value), as shown in Table 4.

Structure and thermochemistry of the intermediates of the methide transfer reactions

Intermediate "mixed" complexes of these methide transfer reactions were not observed in mass-spectrometry experiments, probably due to the fact that fast exothermic dissociation precludes collisional stabilization [5].

Their predicted structures using quantum chemical methods, firstly reported here, are depicted in Fig. 1 (b-d). All three complexes exist as minima (no imaginary frequencies were calculated for them) on the potential energy surfaces of the methide transfer reactions and belong to the C_{3v} pont group.

Contrasting the "symmetric" $[(CH_3)_3Si\text{-}CH_3\text{-}Si(CH_3)_3]^+$ complex (Fig. 1a), the central methyl group in $[(CH_3)_3M\text{-}CH_3\text{-}M'(CH_3)_3]^+$ is not planar and the H-C-H angle in it

Table 5 Theoretical association energies (ΔH^0 in kcal mol^{-1}) of the $[(CH_3)_3M\text{-}CH_3\text{-}M'(CH_3)_3]^+$ complexes (M,M′ = Si,Ge,Sn)

	cc-pVDZ	aug-cc-pVDZ	cc-pVTZ	aug-cc-pVTZ[a]	BSSE[b]
$[(CH_3)_3Si\text{-}CH_3\text{-}Ge(CH_3)_3]^+$					
B3LYP	−22.4	−22.9	−21.7		0.3
BMK	−25.0	−25.6	−25.1	−25.5	0.4
M06L	−27.6	−28.4	−27.4	−27.3	0.6
ωB97XD	−27.6	−28.0	−28.0	−27.3	0.3
G2(MP2)	−28.6				
G3(MP2)	−28.5				
$[(CH_3)_3Si\text{-}CH_3\text{-}Sn(CH_3)_3]^+$					
B3LYP	−28.7	−30.7	−29.6	−30.1	0.5
BMK	−33.2	−36.0	−34.3	−35.7	0.6
M06L	−35.1	−37.6	−35.7	−36.2	0.7
ωB97XD	−35.3	−37.8	−37.1	−37.5	0.5
$[(CH_3)_3Ge\text{-}CH_3\text{-}Sn(CH_3)_3]^+$					
B3LYP	−22.8	−24.4	−23.2	−23.8	0.5
BMK	−25.1	−27.5	−26.3	−27.5	0.6
M06L	−27.5	−29.9	−27.5	−27.9	0.7
ωB97XD	−28.4	−30.6	−30.0	−30.5	0.5

[a] Single-point calculation at the B3LYP/aug-cc-pVTZ optimized geometries with thermal correction to enthalpy at the B3LYP level

[b] Basis set superposition error (kcal mol^{-1}) calculated by a counterpoise method at B3LYP/aug-cc-pVTZ optimized geometries

deviates from 120°, for the M, M′=Si complex, to 116.6° for M=Si, M′=Ge, 114.8° for M=Si, M′=Sn, and 116.2° for M=Ge, M′=Sn. Correspondingly, the NBO charge on M decreases and that on M′ increases along with the planarity of the M′$(CH_3)_3$ group. Thus, in "mixed" $(CH_3)_3$M-CH_3-M′$(CH_3)_3$ intermediates, the structure may be presented as a complex between the M$(CH)_4$ molecule and the $[M'(CH_3)_3]^+$ ion. This fact favors the detachment of $[M'(CH_3)_3]^+$ ions and may be the reason for the fast dissociation of these ions.

Taking into account the comparison of the association energy, i.e., enthalpy of formation, of the $[(CH_3)_3Si\text{-}CH_3\text{-}Si(CH_3)_3]^+$ ion with the experimental value we may predict similar energies for "mixed" ions. For the "symmetric" ion, the closest results were given by BSSE-corrected ωB97XD and M06L methods. For M, M′ = Si, Ge these methods give, respectively, −27.0 and −26.7 kcal mol^{-1}, for M, M′ = Si, Sn −37 and −35.5 kcal mol^{-1}, and for M, M′ = Ge, Sn – 30.0 and −27.2 kcal mol^{-1} (Table 5).

Conclusions

1. The binding energy of trimethylsilylium ion with tetramethylsilane estimated by density functionals BMK, M06L, and ωB97XD are in a good agreement with the experimental value and the G2 theoretical estimation. Popular B3LYP substantially underestimates the reaction enthalpy. Basis set superposition error (BSSE) is small for B3LYP and ωB97XD, but substantially larger for the other two DFT methods employed. The BSSE corrected M06L (−21.6) kcal mol^{-1}) and ωB97XD (−22.9) kcal mol^{-1}) closely bracket the experimental value (−22.3±0.4 kcal mol^{-1}), while G2 and G3 values overestimate it.
2. For the $(CH_3)_3Si^+ + (CH_3)_4Ge \leftrightarrow (CH_3)_4Si + (CH_3)_3Ge^+$ methide transfer reaction, the M06L method along with BMK provide the best fit to G2, G3 and experimental enthalpies.
3. For the reactions with M′ = Sn, three methods (with the exclusion of B3LYP) give results within the chemical accuracy criterion (±1 kcal mol^{-1}).
4. Stuctures of the "mixed" $[(CH_3)_3M\text{-}CH_3\text{-}M'(CH_3)_3]^+$ (M≠M′) methide reaction intermediates of C_{3v} symmetry correspond to energy minima at potential energy surfaces. Their equilibrium structures indicate that they may be better described as $M(CH)_4$—$[M'(CH_3)_3]^+$ complexes. These structures provide their fast decomposition and preclude their observation in experiment. Predicted complexation energies (BSSE corrected M06L/aug-cc-pVTZ values) are −26.7 kcal mol^{-1} for M=Si, M′ = Ge, -35.5 kcal mol^{-1} for M=Si, M′ = Sn, and −27.2 kcal mol^{-1} for M=Ge, M′ = Sn.

References

1. Stone JA (1997) Gas-phase association reactions of trimethylsilylium ($(CH_3)_3Si^+$) with organic bases. Mass Spectrom Rev 16:25–49
2. Potzinger P, Lampe FW (1971) Ion-molecule reactions in dimethylsilane, trimethylsilane, and tetramethylsilane. J Phys Chem 75:13–19
3. Odiorne TJ, Harvey J, Vouros P (1972) Chemical ionization mass spectrometry using tetramethylsilane. J Phys Chem 76:3217–3220
4. Klevan L, Munson B (1974) Gaseous ionic reactions in tetramethylsilane. Int J Mass Spectrom Ion Phys 13:261–268
5. Wojtyniak A, Li X, Stone JA (1987) The formation of $(CH_3)_7Si_2^+$ in $(CH_3)_4Si/CH_4$ mixtures and CH_3^- exchange reactions between $(CH_3)_4Si$, $(CH_3)_4Ge$, and $(CH_3)_4Sn$ studied by high pressure mass spectrometry. Can J Chem 65:2849–2854
6. Dávalos JZ, Herrero R, Abboud JLM, Mó O, Yáñez M (2007) How can a carbon atom be covalently bound to five ligands? The case of $Si_2(CH_3)_7^+$. Angew Chem Int Ed 46:381–385
7. Xavier LA, Pliego JR Jr, Riveros JM (2003) Ligand exchange ion–molecule reactions of simple silyl and germyl cations. Int J Mass Spectrom 228:551–562
8. Fernández I, Uggerud E, Frenking G (2007) Stable pentacoordinate carbocations: structure and bonding. Chem Eur J 13:8620–8626
9. Jursic BS (1999) Energetic and structural properties of silicon dicarbides calculated with complete basis set and hybrid density functional theory methods. J Mol Struct (Theochem) 458:257–261
10. Chandra AK, Nguyen MT (1998) A density functional study of weakly bound hydrogen bonded complexes. Chem Phys 232:299–306
11. Rappe AK, Bernstein ER (2000) Ab Initio calculation of nonbonded interactions: are we there yet? J Phys Chem A 104:6117–6128
12. Tsuzuki S, Luthi HP (2001) Interaction energies of van der Waals and hydrogen bonded systems calculated using density functional theory: assessing the PW91 model. J Chem Phys 114:3949–3957
13. Boese AD, Martin JML (2004) Development of density functionals for thermochemical kinetics. J Chem Phys 121:3405–3416
14. Check CE, Gilbert TM (2005) Progressive systematic underestimation of reaction energies by the B3LYP model as the number of C−C bonds increases: why organic chemists should use multiple DFT models for calculations involving polycarbon hydrocarbons. J Org Chem 70:9828–9834
15. Paier J, Marsman M, Kresse G (2007) Why does the B3LYP hybrid functional fail for metals? J Chem Phys 127:024103
16. Neese F, Hansen A, Wennmohs F, Grimme S (2009) Accurate theoretical chemistry with coupled pair models. Acc Chem Res 42: 641–648
17. Korth M, Grimme S (2009) "Mindless" DFT benchmarking. J Chem Theory Comput 5:993–1003
18. Xu X, Alecu IM, Truhlar DG (2011) How well can modern density functionals predict internuclear distances at transition states? J Chem Theory Comput 7:1667–1676
19. Kruse H, Goerigk L, Grimme S (2012) Why the standard B3LYP/6-31G* model chemistry should not be used in DFT calculations of molecular thermochemistry: understanding and correcting the problem. J Org Chem 77:10824–10834
20. Grimme S (2006) Seemingly simple stereoelectronic effects in alkane isomers and the implications for Kohn–Sham density functional theory. Angew Chem Int Ed 45:4460–4464
21. Grimme S (2011) Density functional theory with London dispersion corrections. WIREs Comput Mol Sci 1:211–228
22. Amin EA, Truhlar DG (2008) Zn coordination chemistry: development of benchmark suites for geometries, dipole moments, and bond dissociation energies and their use to test and validate density functionals and molecular orbital theory. J Chem Theory Comput 4:75–85
23. Zhao Y, Truhlar DG (2009) Benchmark energetic data in a model system for grubbs II metathesis catalysis and their use for the

development, assessment, and validation of electronic structure methods. J Chem Theory Comput 5:324–333
24. Zhao Y, Ng HT, Hanson E (2009) Benchmark data for noncovalent interactions in HCOOH···Benzene complexes and their use for validation of density functionals. J Chem Theory Comput 5:2726–2733
25. Zhang Y, Ma N, Wang W (2012) Assessment of the performance of the M05-class and M06-class functionals for the structure and geometry of the hydrogen-bonded and halogen-bonded complexes. J Theo Comput Chem 11:1165–1173
26. Liu Y, Zhao J, Li F, Chen Z (2013) Appropriate description of intermolecular interactions in the methane hydrates: an assessment of DFT methods. J Comput Chem 34:121–131
27. Hohenstein EG, Chill ST, Sherrill GD (2008) Assessment of the performance of the M05-2X and M06-2X exchange-correlation functionals for noncovalent interactions in biomolecules. J Chem Theory Comput 4:1996–2000
28. Leang SS, Zahariev F, Gordona MS (2012) Benchmarking the performance of time-dependent density functional methods. J Chem Phys 136:104101
29. Grimme S, Steinmetz M, Korth M (2007) How to compute isomerization energies of organic molecules with quantum chemical methods. J Org Chem 72:2118–2126
30. Quintal MM, Karton A, Iron MA, Boese AD, Martin JML (2006) Benchmark study of DFT functionals for late-transition-metal reactions. J Phys Chem A 110:709–716
31. Izgorodina EI, Coote ML, Radom L (2005) Trends in R−X bond dissociation energies (R = Me, Et, i-Pr, t-Bu; X = H, CH3, OCH3, OH, F): a surprising shortcoming of density functional theory. J Phys Chem A 109:7558–7566
32. Zheng W-R, Fu Y, Guo Q-X (2008) G3//BMK and its application to calculation of bond dissociation enthalpies. J Chem Theory Comput 4:1324–1333
33. Wang Y-G (2009) Examination of DFT and TDDFT methods II. J Phys Chem A 113:10873–10879
34. Becke AD (1993) A new mixing of Hartree-Fock and local density-functional theories. J Chem Phys 98:1372–1377
35. Lee C, Yang W, Parr RG (1988) Development of the Colle-Salvetti correlation-energy formula into a functional of the electron density. Phys Rev B 37:785–789
36. Zhao Y, Truhlar DG (2006) A new local density functional for main-group thermochemistry, transition metal bonding, thermochemical kinetics, and noncovalent interactions. J Chem Phys 125:194101
37. Chai J-D, Head-Gordon M (2008) Long-range corrected hybrid density functionals with damped atom–atom dispersion corrections. Phys Chem Chem Phys 10:6615–6620
38. Woon DE, Dunning TH (1993) Gaussian basis sets for use in correlated molecular calculations III. The atoms aluminum through argon. J Chem Phys 98:1358–1371
39. Hay PJ, Wadt WR (1985) Ab initio effective core potentials for molecular calculations. Potentials for the transition metal atoms Sc to Hg. J Chem Phys 82:270–283
40. Hay PJ, Wadt WR (1985) Ab initio effective core potentials for molecular calculations. Potentials for main group elements Na to Bi. J Chem Phys 82:284–298
41. Hay PJ, Wadt WR (1985) Ab initio effective core potentials for molecular calculations. Potentials for K to Au including the outermost core orbitals. J Chem Phys 82:299–310
42. Curtiss LA, Raghavachari K, Trucks GW, Pople JA (1991) Gaussian-2 theory for molecular energies of first- and second-row compounds. J Chem Phys 94:7221–7230
43. Curtiss LA, Raghavachari K, Redfern PC, Rassolov V, Pople JA (1998) Gaussian-3 (G3) theory for molecules containing first and second-row atoms. J Chem Phys 109:7764–7776
44. Frisch MJ et al. (2009) Gaussian 09, Revision B.01, Gaussian Inc., Wallingford
45. Reed AE, Curtiss LA, Weinhold F (1988) Intermolecular interactions from a natural bond orbital, donor-acceptor viewpoint. Chem Rev 88: 899–926
46. Glendening ED, Reed AE, Carpenter JE, Weinhold F (1988) NBO v3.1, Madison
47. Boys SF, Bernardi F (1970) The calculation of small molecular interactions by the differences of separate total energies. Some procedures with reduced errors. Mol Phys 19:553–566